

## Article

# Surface Functionalization of Bamboo with Silver-Reduced Graphene Oxide Nanosheets to Improve Hydrophobicity and Mold Resistance

Dhivyabharathi Balakrishnan <sup>1</sup>  and Cheng-I Lee <sup>1,2,3,\*</sup> 

<sup>1</sup> Department of Biomedical Sciences, National Chung Cheng University, Chia-Yi 62102, Taiwan; d08258005@ccu.edu.tw

<sup>2</sup> Center for Nano Bio-Detections, National Chung Cheng University, Chia-Yi 62102, Taiwan

<sup>3</sup> Advanced Institute of Manufacturing with High-Tech Innovations, National Chung Cheng University, Chia-Yi 62102, Taiwan

\* Correspondence: biocil@ccu.edu.tw

**Abstract:** A natural polyphenolic compound was used to assemble nanocomposites. Owing to its stable bioactive properties, bamboo has earned significant attention in material science. Its high nutrient content and hydrophilicity makes bamboo more vulnerable to mold attacks and shortened shelf lives. To produce efficient, multipurpose, long-life bamboo products, a novel technique involving an immersion dry hydrothermal process was applied to impregnate the bamboo with polyphenol-assisted silver-reduced graphene oxide nanosheets. Curcumin (Cur), a natural polyphenol found in the rhizome of *Curcuma longa*, was used in the preparation of curcumin-enhanced silver-reduced graphene oxide nanosheets (Cur-AgrGONSs). The nanocomposites and nanocomposite-impregnated bamboo materials were examined by field emission scanning electron microscopy, X-ray diffraction and Fourier transform infrared spectroscopy. At the same time, a phytopathogen was isolated from infected bamboo products and identified by internal transcribed spacer (ITS) sequences. The nanocomposites effectively inhibited the growth of the isolated fungus. The mold resistance and moisture content of both the treated and untreated bamboo timbers were also examined to determine the efficiency of the prepared nanocomposite. The antifungal activity and hydrophobicity of the bamboo materials were significantly enhanced after the incorporation of curcumin-enriched silver-loaded reduced graphene oxide nanosheets (B@Cur-AgrGONSs). This research outcome confirms that the nanocomposite is a well-organized antimicrobial material for different advanced domains.

**Keywords:** bamboo susceptibility; mold resistance; graphene silver nanocomposite; antifungal; moisture content; hydrophobicity



**Citation:** Balakrishnan, D.; Lee, C.-I. Surface Functionalization of Bamboo with Silver-Reduced Graphene Oxide Nanosheets to Improve Hydrophobicity and Mold Resistance. *Coatings* **2022**, *12*, 980. <https://doi.org/10.3390/coatings12070980>

Academic Editors: Daniela Predoi, Carmen Steluta Ciobanu and Alina Mihaela Prodan

Received: 6 June 2022

Accepted: 6 July 2022

Published: 11 July 2022

**Publisher's Note:** MDPI stays neutral with regard to jurisdictional claims in published maps and institutional affiliations.



**Copyright:** © 2022 by the authors. Licensee MDPI, Basel, Switzerland. This article is an open access article distributed under the terms and conditions of the Creative Commons Attribution (CC BY) license (<https://creativecommons.org/licenses/by/4.0/>).

## 1. Introduction

Bamboo, a primitive grass (*Poaceae*), is found in large quantities in Asian countries. Bamboo biocomposites are generally composed of cellulose (55%), hemicellulose (20%) and lignin (25%), which are responsible for its mechanical strength [1]. The distribution of its fibers is anisotropic in the longitudinal direction. Its growth is very rapid, with a maximum rate of 22 cm each day [2]. One kind of giant bamboo may reach up to 40 m high in few months. As a result, it has played a significant role in human history, since it has unique innate assets, such as durable mechanical properties, a high strength, an appealing texture, good formability and wide availability [3]. On this account, the use of bamboo has been proposed as an exciting alternative in place of certain composites in various processes used in civil engineering, the textile industry, decoration materials, household products and other industrial processes [4]. As of now, almost a billion individuals live in houses made of bamboo and three billion people depend on this resource for their livelihood [5]. Bamboo and woodlands more generally are easily attacked easily by many species including

*Aspergillus*, *Trichoderma* and *Penicillium* in both industrial and environmental contexts. Metabolites and enzymes produced by those cells are involved in the degradation of the cellulose, lignin and hemicellulose of the bamboo [6]. At the same time, when bamboo products are exposed to an external environment, the starch granules that exist on the parenchymal tissues of bamboo act as a nutrient supplement for the progression of microbes, making them easily prone to the fungal attacks, resulting in a poor decay-resistance [7,8]. The implementation of bamboo has therefore been limited due to its lack of robustness in the face of microbial degradation. The daily usage of natural bamboo and bamboo products has decreased due to its degradation by microbiological activity [6]. Unprotected bamboo materials are easily attacked by the fungal species, bugs, insects and easily become degraded when exposed to moist, polluted air or acid rain or when they suffer long-term exposure to sun-light; thus, the above factors decrease the shelf life and economic value of bamboo products [9]. At this time, the field of nanotechnological research is focused on the use of metal nanoparticles in order to control the microbial populations [10,11]. In order to resolve the above problem and to improve the economic status of bamboo materials, it is essential to formulate a protective coating for bamboo materials by infusion or treatment with nano fillers [12,13].

Graphene is a two-dimensional crystal tightly packed by a monolayer carbon atom. The oxidative derivation of graphene from a carbon group called graphene oxide results in a fascinating material [14]. Many researchers have reported the superior antibacterial properties of graphene papers [15]. Among all the inorganic nanoparticles (NPs) based on gold (Au), silver (Ag) and iron oxide nanoparticles, mesoporous nanoparticles and quantum dots, silver nanoparticles are the most used nanomaterial in different industrial applications and academic research. Silver nanoparticles are known for specific features which act against insects, bacteria and fungi and affect the metabolism of these microorganisms [16,17]. Silver nanoparticles (AgNPs) are disinfectants that can meaningfully reduce many fungal infections for long periods compared with widely-used fungicides [18]. In addition, silver nanoparticles possess the ability to interfere with the metabolisms of microorganisms. Silver nanoparticles that were used to fill up the bamboo matrix could inhibit the proliferation of fungi and thus increase its durability [19]. According to Kim et al., [20], the antifungal performance of silver nanoparticles towards *Candida albicans* was excellent, with complete disruption in terms of cell membrane integrity and thus the collapse of the normal budding process, which led to cell death. At the same time, the researchers also proved that silver nanoparticles not only damage fungal hyphae and that even conidial germination is affected and inhibited, which was also evidenced in phytopathogenic fungi *Raffaella* spp. [21,22]. According to Hamed et al., a low concentration of silver nanoparticles effectively inhibited the growth and survival of *Penicillium chrysogenum* and *Aspergillus niger* strains [6]. Many studies have explained the theoretical mechanism of the relationship between fungi and silver and reported low to moderate resistance to brown-rot fungi in wood treated with silver salts [23]. High preservation efficiencies were noted for wood treated with AgNPs of various absorptions (200 and 400 ppm) with respect to the white-rot fungus *Tinea versicolor* [24]. However, Akhtari and Arefkhani found that micronized metals such as silver, gold, titanium and zinc were very effective in preventing mass loss and *Tinea versicolor* cell degradation after 4 months [25]. Overall, AgNPs have garnered significant attention since they are effective against numerous kinds of bacteria, fungi and viruses [26,27]. A member of the Zingiberaceae family, *Curcuma longa* has received a great deal of attention in the production of many complex compounds such as curcumenol, curdione, curcumin, isocurcumenol and curcumol. These groups have been reported to have toxic effects on fungi involved in the deterioration of agricultural products by interfering with mycelial development [28]. In addition, curcumin dye has high adhesion characteristics, that is, the ability to adhere to any substrate surface [29]. The combination of different nanocomposites reduces the cost of production. At the same time, product yield increases along with synergistic potential. GO nanosheets possess a two-dimensional structure with a large surface area with different oxygen groups such as OH and COOH [30]. These oxygens, which

contain functional groups, enhance the adhesion of GO and bamboo. Wang et al. introduced graphene oxide nanosheets to bamboo using the heat press treatment to improve its mechanical properties. In this research, it was found that the graphene is a good carrier and supporting material for loading and releasing the nanomaterials in the target [31]. Li et al. revealed that Fe-doped TiO<sub>2</sub>/bamboo demonstrated a higher photocatalytic disinfection rate with respect to fungi in comparison with TiO<sub>2</sub>/bamboo. Together with an increase in the efficiency of the Fe dopants of the electron-hole pair, separation was increased and thus the antifungal properties of the material were enhanced even in natural light [32]. Liu et al. incorporated silver nanoparticles into TiO<sub>2</sub> nanoparticles. This combination resulted in enhanced photocatalytic activity under visible light. However, the plain TiO<sub>2</sub> was found to be very inefficient, with a narrow photoreaction range [33]. However, these drawbacks were minimized by integrating the particles with other metals such as Ag [33–35], Cu [36], Fe [37], Zn [38–40] and SiO<sub>2</sub> [31]. Taking into account both the costs and effects, the combination of GO with metal nanoparticles is considered a superior and suitable material in the context of bamboo modification [27]. So far, a number of studies have been carried on the nano-modification of bamboo to improve its shelf life, as shown in Table 1.

**Table 1.** Nanotechnology in bamboo modification and its utilization effects.

Nanomaterials	Process	Effect	Ref.
rGO	Ultrasonic dispersion and hydrothermal reduction	Improved bamboo decay resistance	Wang et al. [27]
GO-SiO <sub>2</sub>	SiO <sub>2</sub> sprayed on GO-bamboo	Improved hydrophobicity and dimensional stability	Wang et al. [31]
Fe-doped TiO <sub>2</sub> films	Deposited using the co-precipitation method on bamboo surface and doping carried via the immersion of bamboo in nano suspension	Improved antifungal activity	Li et al. [32]
Ag/TiO <sub>2</sub>	Ag and TiO <sub>2</sub> nanoparticles being immobilized on the surface of polydopamine-bamboo composite via impregnation-adsorption and in situ growth	Anti-mildew property	Liu et al. [33]
Ag/TiO <sub>2</sub>	Hydrothermal immobilization of TiO <sub>2</sub> on bamboo and AgNPs embedded on TiO <sub>2</sub> films	Superior antifungal activity and complete inhibition of <i>T. viride</i> and <i>P. citrinum</i>	Li et al. [34]
Ag nanogel	Impregnation treatment	Long-term antifungal effect; mildew resistance against <i>A. niger</i>	Yu et al. [35]
PMS/CuNP	Bamboo immersed in alkaline SMS and acidic CuCl <sub>2</sub> solution and dried at 103° for 2 h	Increased hydrophobicity, with an anti-mildew effect	Wang et al. [36]
Fe <sub>3</sub> O <sub>4</sub>	Co-precipitation and deposition	Improved hydrophobic properties, with a water contact angle of 116.8°	Lou et al. [37]
ZnO	Colloidal deposition of ZnO and wet chemical treatment	Resistant against <i>A. niger</i> and <i>P. citrinum</i> ; weaker resistance against <i>T. viride</i>	Li et al. [38]
ZnO/PMHS	Dip dry and hydrothermal treatment	Synergistic antifungal activity by ZnO and PMHS	Chen et al. [39]
ZnO-TiO <sub>2</sub>	Liquid phase deposition	Improved thermal stability, with a flame-retardant property	Ren et al. [40]
AgNPs	Impregnation of bamboo in AgNPs colloidal solution	Inhibition of fungal proliferation	Pandoli et al. [41]

By comparing these studies, silver nanoparticles can be considered to be a better coating agent, with superior antimicrobial properties [41]. The use of a graphene-incorporated silver nanocoating is an effective way to improve the decay resistance of bamboo. This research reports an impregnation method for self-assembly of Cur-AgrGONSs onto the surface of bamboo through an immersion dry hydrothermal process. The decay and mold

resistance of the bamboo sample produced was determined. In addition, the micromorphology, crystalline phase, microstructure and other physicochemical properties of the coating were investigated. This research will provide a scientific foundation for investigation into the anti-mold mechanisms of Cur-AgrGONSs on wood surfaces and guide the application of nanocomposites in the field of wood antimicrobials.

## 2. Materials and Methods

### 2.1. Isolation and Identification of Bamboo-Decaying Fungi

For the isolation of fungal pathogens, bamboo blocks and small decorative materials made of bamboo were obtained from Puyuan Art Company (Nantou, Taiwan). The most visibly decayed bamboo materials were cut into small blocks. Further, surface sterilization was performed for the bamboo samples by means of washing for 1 min in 70% ethanol and immersion in a solution of 3% sodium hypochlorite for 3 min, followed by an ethanol rinse for 30 s. Later, the blocks were rinsed in milli-Q water and dried with sterile tissue paper. The dried blocks were positioned on malt extract agar medium, and the medium was supplemented with 100 µg/mL of streptomycin to inhibit the growth of bacteria. The incubation of the plates were carried out for 2 weeks at temperatures below 27 °C. Every single fungus was purified, and the colonies of fungi were classified according to colony-formation characteristic features such as shape, surface, opacity, margins and chromogenesis. The DNA was immediately isolated from an actively grown mycelium mat around the inoculated blocks using malt extract agar (MEA) plates. Electrophoresis was performed on an 0.8% agarose gel to separate the DNA bands [42]. With the aim of amplifying the polymerase chain reaction (PCR), primers ITS-1 and ITS-4 were applied for the analysis of fungal ITS sequences. After the addition of Taq polymerase, the reaction mixture for PCR was obtained. After the reaction, the PCR products were proceeded for purification and sequenced [43]. The sequences were aligned, and their closely related sequences were determined using a BLAST search [44]. The CLUSTAL W program was used for multiple sequence alignment. A phylogenetic genogram was constructed by the neighbor joining method using the software MEGA, version 10.0 [45].

### 2.2. Graphene Oxide (GO) Synthesis

GO was prepared using the Hummers method with trivial modifications by means of employing the blend of sulfuric acid (H<sub>2</sub>SO<sub>4</sub>) and potassium permanganate (KMnO<sub>4</sub>) [46]. Briefly, fine graphite flakes were continuously blended in concentrated H<sub>2</sub>SO<sub>4</sub> (98%) for 2 h. The reaction was maintained at below 20 °C. Gradually, KMnO<sub>4</sub> was added into the overhead mixture. The reaction mixture was stirred for 1 h at 35 °C. Later, distilled water was added, followed by stirring for 1 h to attain a dark brown suspension. A visibly bright yellow layer was obtained with the addition of 30% hydrogen peroxide solution. Lastly, graphene oxide was obtained by repeated spinning at a speed of 10,000 rpm for 15 min with 5% HCl followed by distilled water with the aim of neutralizing the pH, which was later confirmed with a pH meter. Furthermore, the GO was washed to remove impurities and to eliminate excess manganese.

### 2.3. Preparation of Cur-AgrGO Nanosheets

The reaction was performed by preparing a mixture of 1 mM Cur and 60 mg of GO in distilled water. The pH was raised to 9 with the help of 5 M ammonia solution. At the same time, 2 mM of silver nitrate was added drop wise. Throughout the whole synthesis period, the pH was maintained at 9. Then, the reaction was maintained at 90 °C for 1 h. The composites were separated and washed three times via centrifugation for 15 min at 10,000 rpm. The concentrated pellet was lyophilized to obtain the nanocomposites in the form of a pure fine powder.

#### 2.4. Preparation of Cur-AgrGONSs-Impregnated Mold-Resistant Bamboo Samples

The bamboo blocks were placed into a beaker containing 50 mL of colloidal solution of Cur-AgrGONSs. It was subjected to five impregnation cycles through an immersion dry hydrothermal process. A fresh colloidal solution of Cur-AgrGONSs was used for each cycle. The final products were rinsed with deionized water for the removal of unattached and free GO nanosheets and dried at 50 °C for overnight to remove the wetness.

#### 2.5. Characterization of Cur-AgrGO Nanosheets

The morphological characterization and elemental composition analysis of the GO, rGO and Cur-AgrGONSs was performed by field emission scanning electron microscopy with an attached EDX (FE-SEM/EDX, Hitachi S4800-I, Tokyo, Japan; acceleration voltage: 0.1 to 30 KV) and transmission electron microscopy (TEM, JEM-2010, JEOL, Tokyo, Japan, acceleration voltage: 200 KV). Its crystalline nature was studied by X-ray diffraction (Bruker AXS GmbH instrument, Nanostar U System, Karlsruhe, Germany) using Cu K $\alpha$  radiation with 40 KV and 40 mA, ranging from 5° to 80° at a 2 $\theta$  scan rate of 4° min<sup>-1</sup>. The UV–visible spectroscopy was performed in the range of 200–800 nm (SCINCO S-3100, Seoul, Korea). Fourier-transform infrared (FTIR) spectroscopy was performed with an FTIR spectrometer (VERTEX 70V, Bruker, Norwalk, CT, USA) to identify the existence of the functional groups.

#### 2.6. Mold-Resistant Test

A quick and accessible method was employed for the assessment of antifungal properties. Compared to the common wood, bamboo harbors mold, which grows very rapidly in a higher moisture environment and makes the fungal inoculation of the bamboo needless, whereas it is typically essential for wood materials [47]. The bamboo samples were prepared as blocks and their surfaces were sterilized with 70% alcohol and water. Untreated bamboo and bamboo incorporated with GO and Cur-AgrGONSs were placed in a potato dextrose agar (PDA) medium inoculated with the isolated fungal species. The plates were maintained at 25–27 °C for 30 d with 95% humidity. During the incubation period, the diameters of the fungal colonies which had grown was measured weekly and the rate of mold inhibition was calculated using the formula provided below.

$$\text{Mold inhibition rate (\%)} = (\text{DC} - \text{DT}/\text{DC}) \times 100$$

where DC is the diameter (mm) of mycelium grown in the untreated plate and DT is the average diameter (mm) of the mycelial colonies grown in the treated plate.

#### 2.7. Moisture Content Evaluation by Water Absorption Test

The experiments were performed by immersing both the control and treated specimens in water at room temperature for 70 h and assessing the moisture content level (%) of the immersed samples. The following equation was used to calculate the moisture content percentage of the samples:

$$\text{Moisture content (\%)} = (\text{specimen weight} - \text{dry weight})/\text{dry weight}$$

The dry weight, however, was attained by drying the bamboo samples at 105 °C.

#### 2.8. Water Contact Angle (WCA) Test

The main physical characteristics of bamboo materials are their water absorption properties, which determine their applications [48]. Both the pristine bamboo and treated bamboo were subjected to the WCA test. This was assessed on a contact angle surveyor (CAM-100, Ding Ding Nanotechnology, Taichung, Taiwan). WCAs were measured after the water droplets contacted the surfaces of both the treated and untreated samples. The absolute significance of the WCA tests was obtained as an average of five measurements [49,50].

### 2.9. In Vitro Decay Test

A bamboo decay test was performed based on the protocol developed by the American Society for Testing and Materials [51], with minor modifications. This experiment also aims to measure the percentage of the weight of the bamboo material lost as a result of the decay process. Fungal mycelium was grown on 2% malt extract broth for 1 week prior to the inoculation of the bamboo blocks into the medium. The bamboo blocks of 50 mm × 20 mm × 5 mm were cut from the logs, were cleaned by means of surface sterilization, dried for one hour and weighed before being introduced into the mycelium-grown medium. The same procedure was followed for the two different isolated fungi. After the inoculation of the bamboo blocks onto the medium, the medium was maintained at  $22 \pm 1$  °C with the relative humidity of  $70\% \pm 5\%$  for 12 weeks. The amount of weight lost was checked by removing the samples from the medium. The mycelium grown on the fungi was completely brushed off and hot dried at 80–100 °C for 12 h and finally weighed to determine the weight lost [52].

### 2.10. Antifungal Activity

The antifungal efficiency of the produced nanocomposite was assessed through the inhibition of mycelium growth assay by directly infusing Cur-AgrGONSs in potato dextrose agar medium [53]. *Penicillium funiculosum* and *Trichoderma afroharzianum* were grown in a PDA medium for 5 d at 28 °C. After 5 d of incubation, the spores obtained were collected and maintained under lights for 5 d with moderate shaking to obtain the suspension of microconidia. The micro conidial suspension was filtered using sterilized gauze. In order to harvest the conidia, centrifugation was performed at 5000 rpm for 5 min and the suspension was twice washed with distilled water. The suspension of the spores was adjusted to a concentration of  $3 \times 10^7$  spores/mL and inoculated on PDA plates containing different concentrations of Cur-AgrGONSs (0, 1, 5, 10, 25, 50, 75, 100 µg/mL). The plates were incubated for 7 d at 25 °C. The experimentations were carried in a triplicate manner and the average diameter of the fungal colonies was determined. The inhibition of mycelial progression of *Penicillium funiculosum* and *Trichoderma afroharzianum* was proportionate to the nanocomposite concentrations from 0–100 µg/mL in the nutrient media. The potential anti-mold efficiency was quantified as a percentage using the equation [54]:

$$\text{Inhibition of mycelial growth (\%)} = ((DC - DT)/DC) \times 100$$

where DC is the mediocre diameter (mm) of the mycelial colony formed in the untreated plate and DT is the average diameter (mm) of the mycelial colony on the treated plate.

## 3. Results and Discussion

The fungal pathogens isolated from the bamboo blocks were identified. The chemical and physical properties of the synthesized Cur-AgrGONSs were characterized. Finally, the antifungal activity of Cur-AgrGONSs against isolated fungi was tested.

### 3.1. Bamboo Decaying Fungi Isolation and Molecular Characterization

In this study, two fungal isolates were obtained from industrially used bamboo materials. A microscopic and macroscopic view is presented in the Figure 1. The two isolated fungi are filamentous fungi which are found on plant roots and reside in soils and play an important role in decaying plant residues [43]. Their conidial and mycelial morphology was identified using the lactophenol cotton blue staining method. Figure 1a,b is characterized as *T. afroharzianum*, with the formation of dense green conidia reaching the edge of the plate after a week incubation. The conidia abundance suppressed the mycelia in the culture. In *T. afroharzianum*, the main branches of conidia were held in pairs and in a coil of phialides. Figure 1c,d is characterized as *P. funiculosum*, with creamy yellow and light-green, densely covered filaments on the plates.

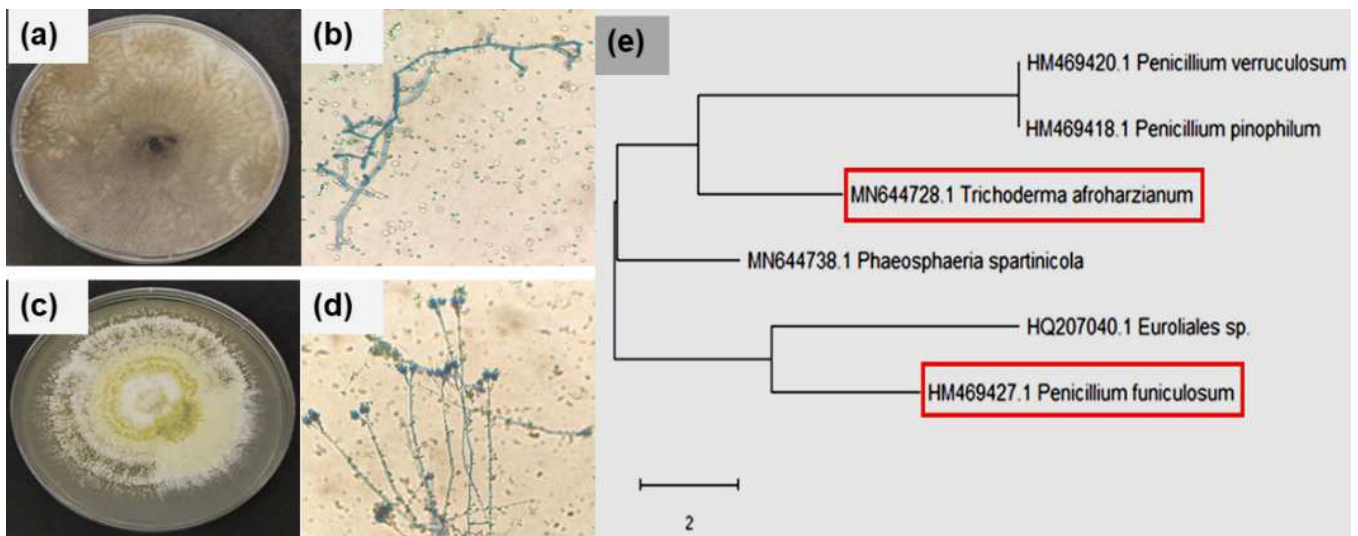


**Figure 1.** (a,c) Two fungal strains isolated from *Phyllostachys edulis* bamboo species. (b,d) Morphology of the isolated strains. (e) Phylogenetic tree of isolated fungal communities.

### 3.2. Preparation of Graphene Oxide and Cur-AgrGONSs

The transformation of natural graphite into GO was achieved using the synthesis of Cur-AgrGONSs. Concerning the preparation of the nanocomposites, Ag ions were first loaded onto the GO surface. They were then reduced and stabilized by polyphenol curcumin, resulting in the assembly of multifaceted Cur-AgrGONSs. Figure 2 represents a schematic illustration of the preparation of nanocomposites through the oxidation reduction method.

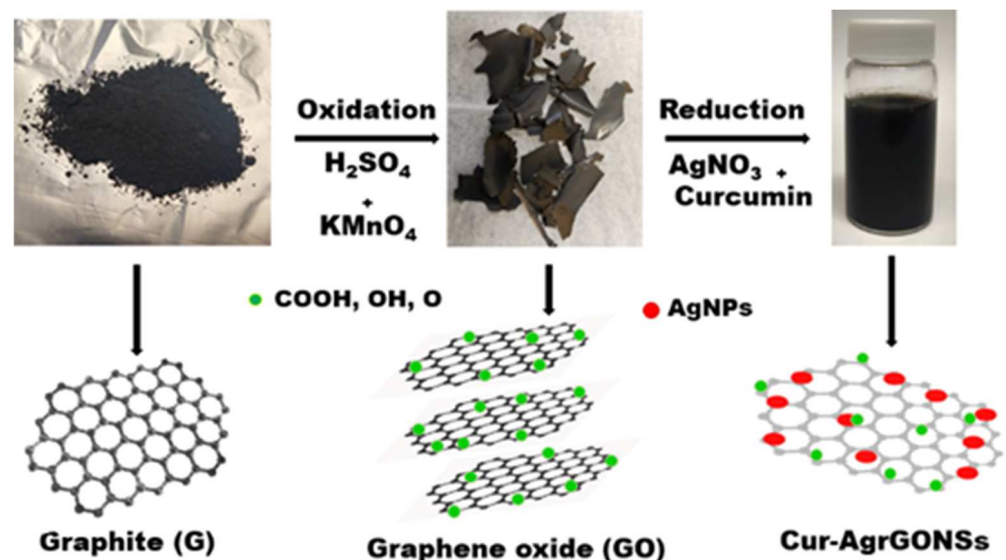


**Figure 2.** A scheme for the preparation of GO and synthesis of Cur-AgrGONSs.

### 3.3. Hybridization of Bamboo with Cur-AgrGONSs

The impregnation enables the silver collections to be intensively deposited in the parenchyma tissues of bamboo cells [55]. Figure 3 provides longitudinal and transverse cross sections of pristine bamboo and bamboo impregnated with Cur-AgrGONSs. Figure 3a–c is the surface morphology of the pristine bamboo using low to high magnification. Bamboo tissue mainly consists of parenchyma cells, vascular bundles composed of metaxylem vessels, sieve tubes and fibers. In Figure 3a,c, radial sections of the bamboo ma-

terial clearly shows the vessels and pits, and the parenchymal cells are shown in Figure 3b, indicated by red arrows. These surfaces show the presence of a rough pore structure [33]. The pores on the pits in Figure 3a are occupied by high amount of nutrients such as sugars and starch. These surfaces allow moisture and air to enter easily and result in the rapid growth of mold by sourcing its nutrients. As shown in Figure 3d–i, the surface of the bamboo was covered through the layered assembly of Cur-AgrGONSs in the initial step via immersion. This GO coating enabled the strong adhesion of silver nanomaterials in the form of seeds. More silver nanoparticles were bound to the surface of the bamboo materials after the three repeated of dip-dry and hydrothermal processes. Vascular bundles and parenchymal pits were abundantly bedded with the Cur-AgrGONSs. Imaging at higher to lower magnifications revealed the crystalline deposition of nanocomposites on the surface of the bamboo. This surface modification helps to improve the material's superhydrophobic properties. The treated bamboo can be exposed to air and humidity for longer period, i.e., months, and to be liberated from contagious settlements. However, the nontreated specimens remained vulnerable to major deterioration.

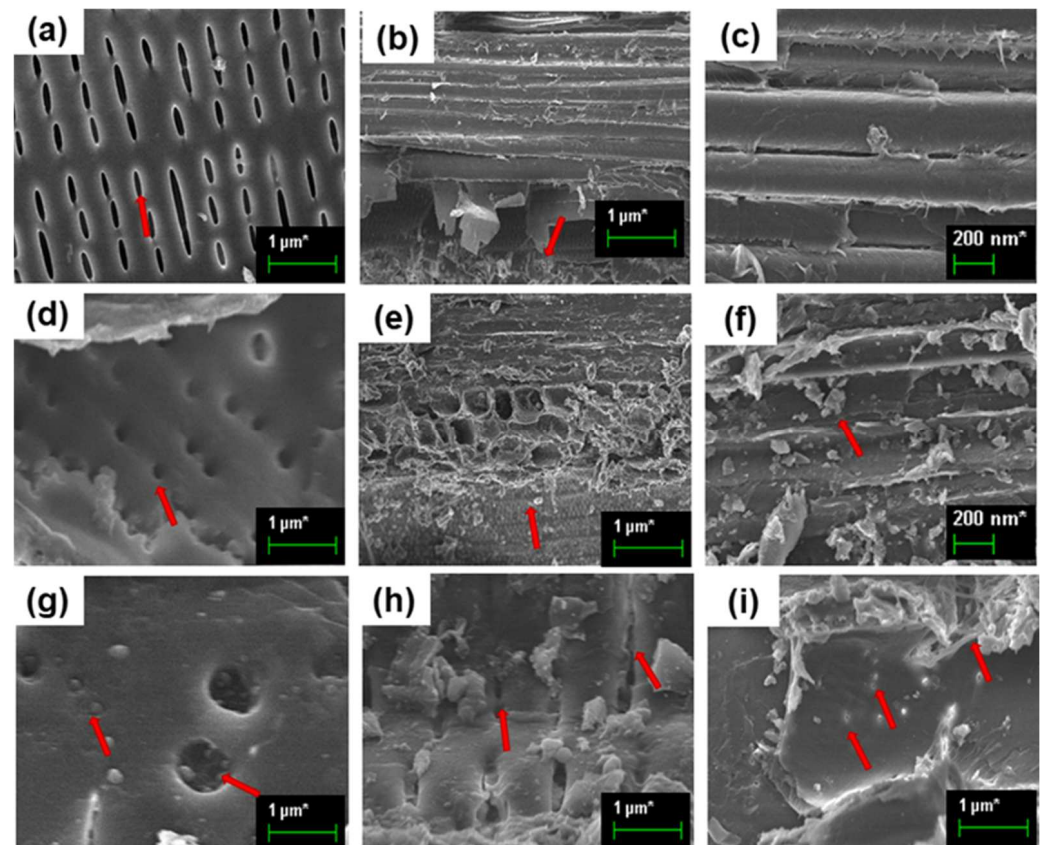


**Figure 3.** (a–c) Morphology of pristine bamboo, (d–i) Cur-AgrGONS-impregnated bamboo vesicles and parenchyma cells (red arrows indicate the deposition and penetration of graphene silver nanoparticles into bamboo cells).

### 3.4. Characterization of Synthesized Cur-AgrGONSs

The UV-Vis spectra of graphite (G), GO, Cur, reduced graphene oxide (rGO) and Cur-AgrGONSs are provided in Figure 4a. As shown, it is known that the UV-Vis spectrum of G has a minor peak at 215 nm. However, GO's maximum absorption peak was at approximately 230 nm. The absorption peak for GO was obtained at 230 nm with respect to the  $n-\pi^*$  and  $\pi-\pi$  transitions of the C–O and C–C bonds. Compared with the typical peak of GO at 230 nm, rGO displayed an absorption peak at approximately 250 nm accompanied by a shoulder peak at approximately 360 nm, suggesting a successful reduction in GO.

For Cur-AgrGONSs, the redshift observed at 250 nm associated with aromatic C–C bonds ( $\pi$ – $\pi^*$  transitions) underscores the formation of Cur-reduced graphene oxide nanosheets with restored C–C bonds. A broad intense peak was obtained at 430 nm and was attributed to the surface plasmon resonance (SPR) effect of AgNPs [56]. The diffraction planes of pristine bamboo and bamboo impregnated with Cur-AgrGONSs was obtained by performing X-ray diffraction analysis. The XRD pattern of the untreated bamboo exhibited sharp crystalline peaks at approximately  $32.3^\circ$ ,  $38.4^\circ$  and  $46.8^\circ$  corresponding to (101), (002) and (004) respectively. These peaks indicated the presence of highly crystalline natural cellulose [57,58]. Figure 4b provides the crystalline pattern of the bamboo treated with Cur-AgrGONSs observed at  $2\theta$  values of  $22.1^\circ$ ,  $28.7^\circ$ ,  $33.8^\circ$ ,  $39.9^\circ$ ,  $45.2^\circ$ ,  $46.1^\circ$ ,  $56.3^\circ$ ,  $57.2^\circ$  and  $79.51^\circ$ , which correspond to hkl planes of (100), (002), (101), (102), (103), (110), (112), (110) and (211) face-centered cubic (fcc) lattice Ag (JCPDS-04-0783). The diffraction intensity increased upon treatment with the bio-functionalized nanosheets. Generally, this reaction takes place in the amorphous regions [59].

As shown in Figure 4c, Cur-AgrGONSs underwent significant IR transmission at  $3125$ ,  $1589$ ,  $1514$ ,  $1367$ ,  $1024$  and  $818$   $\text{cm}^{-1}$ . The solid peaks of  $3125$  and  $1589$   $\text{cm}^{-1}$  can be attributed to C–C stretches, and the wide peaks of  $1514$   $\text{cm}^{-1}$  correspond to hydroxyl (O–H) functional groups. The  $1024$   $\text{cm}^{-1}$  band can be attributed to C–O–C and C–O stretch modes. Figure 4d shows the surface morphology of GO and Cur-AgrGONSs assessed by FE-SEM and TEM. Raman spectroscopy is one of the most influential and helpful techniques used to study disorder  $\text{sp}^2$  carbon material. In Figure 4d, the GO spectrum is characterized by the incidence of a D band at  $1337$   $\text{cm}^{-1}$ ,  $\kappa$ -point phonons with  $A_{1g}$  symmetry to the breathing mode and a G band at  $1606$   $\text{cm}^{-1}$  attributed to the  $E_{2g}$  phonon of the carbon  $\text{sp}^2$  atoms with a tangential stretching mode [60]. The attachment of hydroxyl and epoxide groups to the carbon basal plane causes structural imperfections and thus results in the formation of the D peak. In the Cur-AgrGONSs spectrum, the deposition of AgNPs on the graphene surface causes a difference in intensity in the case of both the D and G bands [61]. The increase in the peak intensity can be attributed to the surface-enhanced Raman scattering (SERS) effect [62].

Figure 4e(i,iv) presents both the FE-SEM image and TEM image of the graphene oxide. The GO layer loaded with silver nanoparticles, which is approximately 25 nm in size, is seen clearly in Figure 4e(iii inset). The TEM results show that a single-layer, sheet-like morphology and a number of crumples appeared at the sheet edges caused by the  $\text{sp}^3$  hybrid bond of carbon atoms during the Hummer's oxidation reaction. Figure 4e(ii,v) shows the surface morphology of rGO. Upon reduction, the layered graphene sheets of a carbonaceous structure break and generate crumples that are visible as clear stacked wrinkles on its surface, with such rough surfaces enhancing the hydrophobic nature of the material. Figure 4e(iii,vi) shows a plain GO nanosheet loaded with the monodispersed AgNPs with sizes ranging from 5–25 nm. Both the FE-SEM and TEM images revealed that a high concentration of small silver nanoparticles with good dispersity was incorporated onto the single layered graphene oxide nanosheets.

The reduction of graphene oxide and successful deposition of silver nanoparticles on the surface of reduced graphene oxide sheets was further confirmed by EDX analysis. Figure 4f(i–iii) shows the elemental compositions of GO, rGO and Cur-AgrGONSs, respectively. In Figure 4f(i), carbon and oxygen signals were derived from the surface of GO. After the reduction process, decreased amounts of the oxygen group in rGO indicated the reduction of oxygenated functional moieties. Figure 4f(ii) also indicates that the hydrophilic graphene was transformed in terms of its hydrophobic nature. The elemental composition of the Cur-AgrGONSs composite was also analyzed by EDX, as shown in Figure 4f(iii). In our measurements, multiple intense peaks for Ag demonstrated that a higher amount of monodispersed silver nanoparticles were deposited and absorbed by the reduced graphene surface.

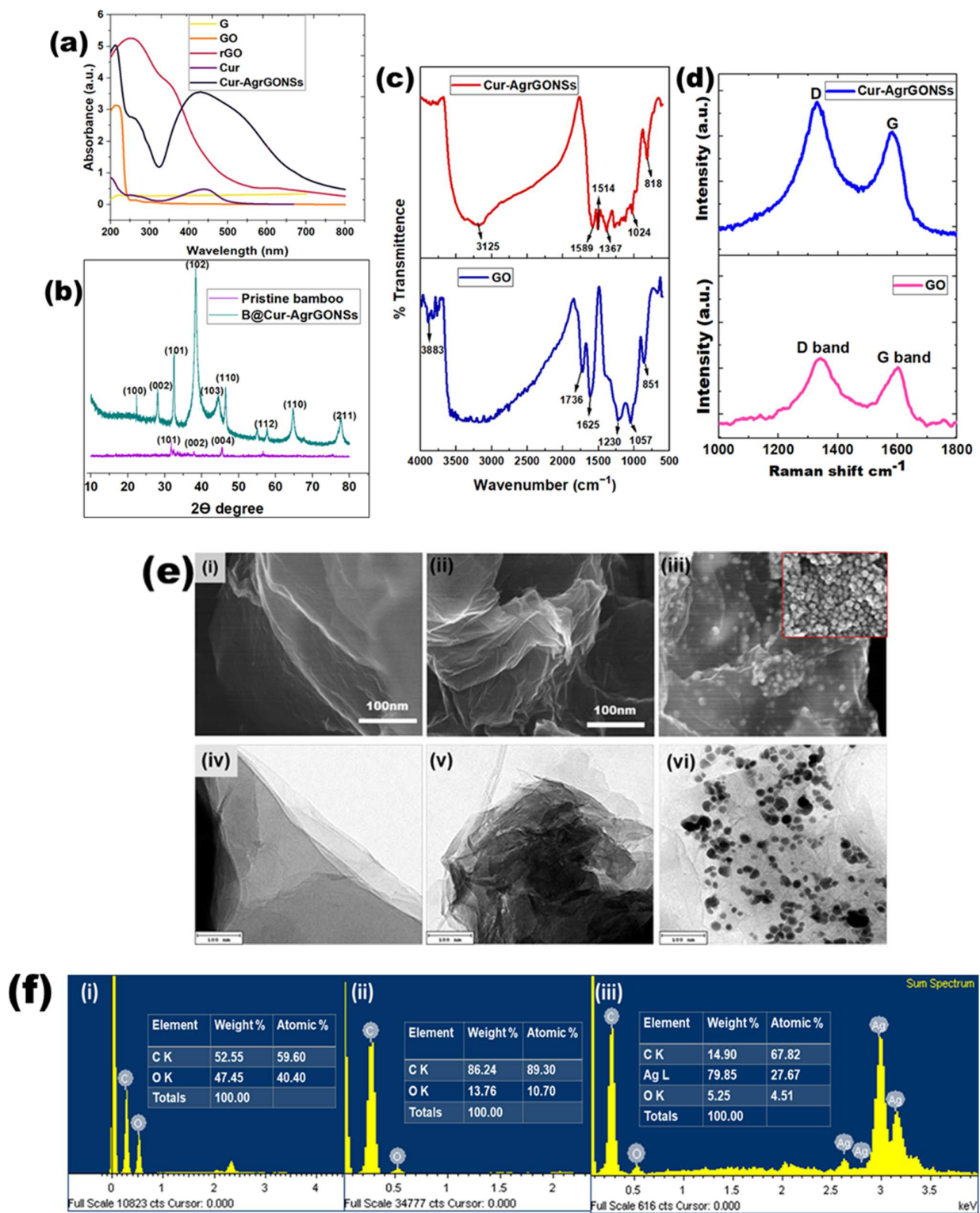


**Figure 4.** (a) UV-vis spectra of G, GO, Cur, rGO and Cur-AgrGO nanosheets. (b) XRD measurements of pristine bamboo and Cur-AgrGONSs impregnated bamboo. (c) FTIR spectroscopy of GO and Cur-AgrGO nanosheets. (d) Raman spectroscopy of GO and Cur-AgrGO nanosheets. (e) (i–iii) FE-SEM of GO, rGO and Cur-AgrGONSs, respectively; (iv–vi) TEM of GO, rGO and Cur-AgrGONSs, respectively. (f) (i–iii) EDX spectra of GO, rGO and Cur-AgrGONSs, respectively.

### 3.5. Mold Resistant Test

A mold resistance test was performed for both the untreated bamboo and treated bamboo samples. According to the standard method (ASTM D3273-21), the experiment was carried out for 30 d. The 30-day incubation time enables molds to mature and sporulate, thus aiding their identification. Figure 5 shows the mold resistance properties of the bamboo materials before and after the incorporation of Cur-AgrGONSs. The pristine bamboo material did not show any kind of resistance towards the phytopathogens, and the molds grew and covered the whole surface due to the high amount of sugar and starch content in the bamboo. In contrast, the bamboo incorporated with GO (B@GO) showed a partial resistance and decreased mold growth when observed in comparison to the nontreated group. The B@Cur-AgrGONSs group showed good resistance towards the fungus. The pristine bamboo was 99% infected with the mycelium of *P. funiculosus* and *T. afroharzianum*. In the first two weeks of observation, the bamboo samples containing Cur-AgrGONSs did not show any mycelium growth and there as a 20% reduction in terms of the infection area with respect to the B@GO after one month of test period. The antimicrobial activity of Cur-AgrGONSs was attributed to the graphene oxide nanosheets and the silver nanoparticles. This kind of synergistic importance with respect to the hydrophobic surfaces of antimicrobial materials was reported earlier [39].

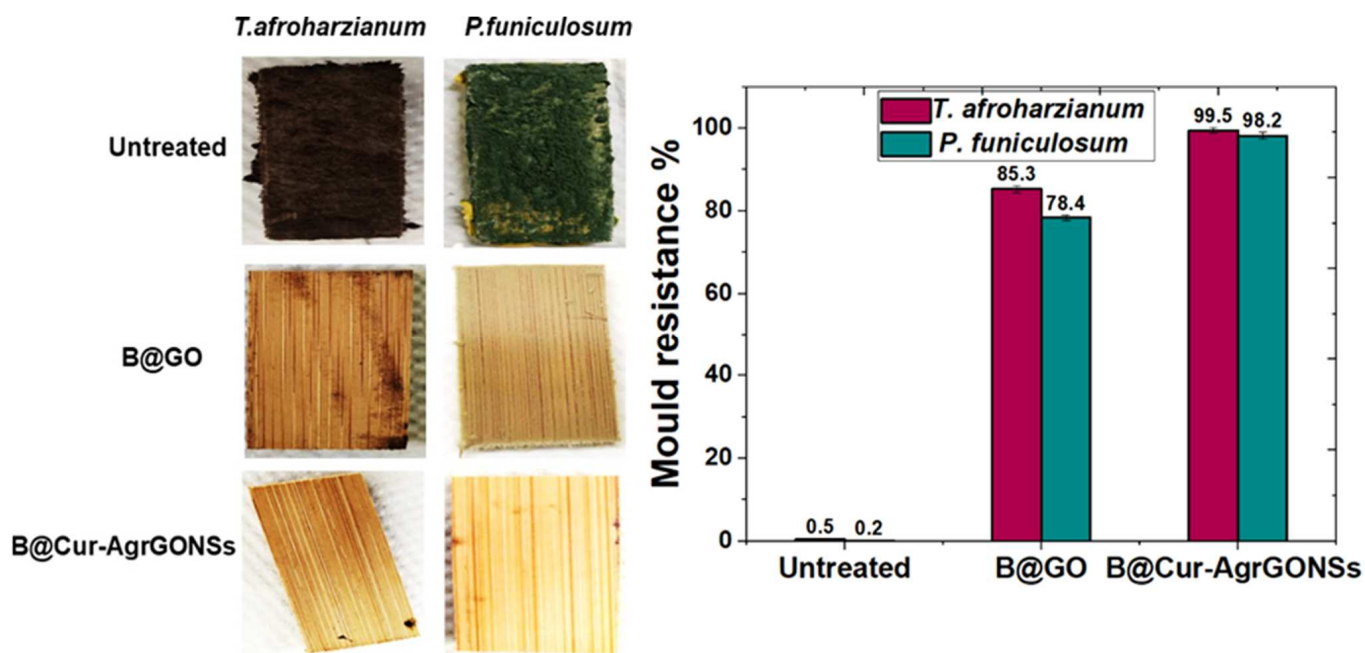


**Figure 5.** Mold resistance performance of pristine bamboo and bamboo impregnated with Cur-AgrGO nanosheets.

### 3.6. Evaluation of Moisture Content and Water Contact Angle by Water Absorption Test

The absorption of water is one of the most significant features of bamboo materials exposed to ecological circumstances that determine their eventual applications [63]. In this investigation, the water resistance properties of the pristine bamboo and B@Cur-AgrGONSs were examined. It was found that the moisture content of the untreated pristine bamboo increased to 98.2% after the specimen was fully immersed in water for 70 h, whereas the moisture level of the treated bamboo remained at approximately 20%–40% with respect to shortest to longest immersion times, as shown in Figure 6a. Such hydrophobicity was achieved by the hydrothermal coating of hydrophobic Cur-AgrGONSs on the surface of pristine bamboo. Furthermore, this characteristic property enhances the shelf life of the material and adds to its value.

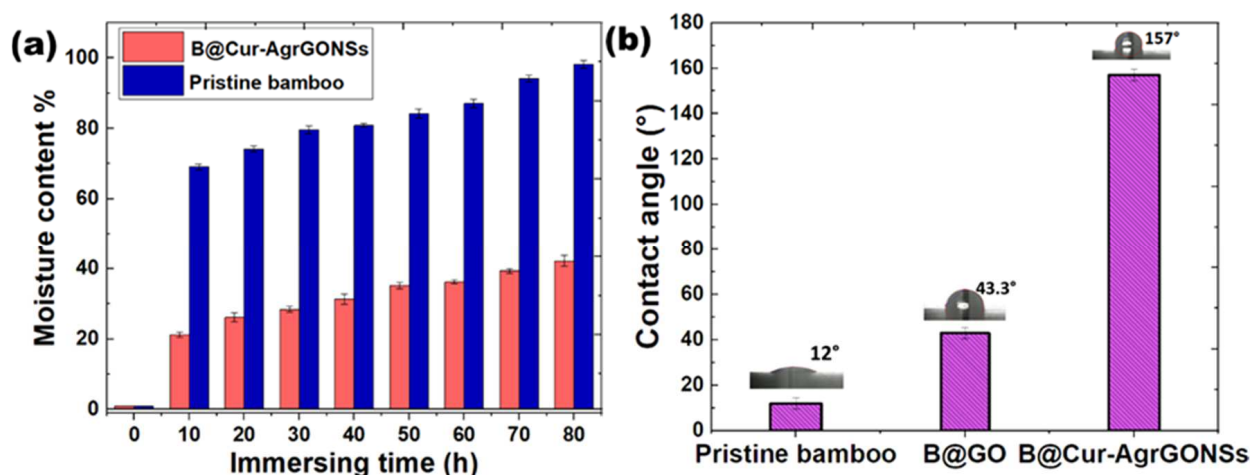


**Figure 6.** (a) Moisture content of pristine bamboo and B@Cur-AgrGONSs. (b) Water contact angle of pristine bamboo, B@GO and B@Cur-AgrGONSs.

In addition, the WCA was also used to characterize the hydrophobicity of the bamboo material impregnated with Cur-AgrGONSs. After 70 h of being immersed in water, the WCA showed that the B@Cur-AgrGONSs had very high level of water resistance, which was consistent with the moisture content test. Figure 6b shows an image of water droplets in a radial cross section of pristine bamboo, where the observed contact angle was only 12°. The quick spread of water over a large surface area and the absorption of water droplets indicates the bamboo material was inherently very hydrophilic as the surface was rich in hydroxyl groups. Therefore, water molecules easily penetrated the pristine bamboo and resulted in aiding the growth of microorganisms in internal spaces. In order to overcome this issue, GO and Cur-AgrGONSs were used to coat and impregnate the bamboo to improve its hydrophobicity. After the deposition of GO and Cur-AgrGO nanosheets by using the hydrothermal process, the crystallization of the nanocomposites on the surface increased the WCAs to 43.3° and 157°, respectively. The significant increase in WCA indicates an improvement in hydrophobicity. Such a level of hydrophobicity not only inhibits the attachment of microorganisms but it also prevents bamboo from absorbing water and other form of liquids such as tea [64]. Due to their resistance to water, Cur-AgrGONSs have been shown to have great potential when used in high humidity environments. The treated bamboo substrate showed not only superior hydrophobicity but also stable repulsion properties.

### 3.7. In Vitro Bamboo Decay Test

Figure 7 represents the average weight lost in terms of pristine bamboo and Cur-AgrGONS-impregnated bamboo samples caused by *P. funiculosum* or *T. afroharzianum* for 84 d. Compared to the weight loss of untreated bamboo samples, that of the samples with Cur-AgrGONSs significantly decreased. For the samples degraded for 84 d, the percentage mass lost was greater in the case of *T. afroharzianum* than *P. funiculosum*. Impregnation with Cur-AgrGONSs is effective in preventing fungal deterioration. In addition, hydrophobicity was achieved by coating the surface of bamboo with Cur-AgrGONSs, making it is possible for the material to suppress the growth of the above two types of pathogens and potentially extend the life of bamboo products. The bamboo material showed a significant difference ( $p = 0.05$ ,  $t$ -test) in terms of its resistance to fungal attack, regardless of fungal species [65].

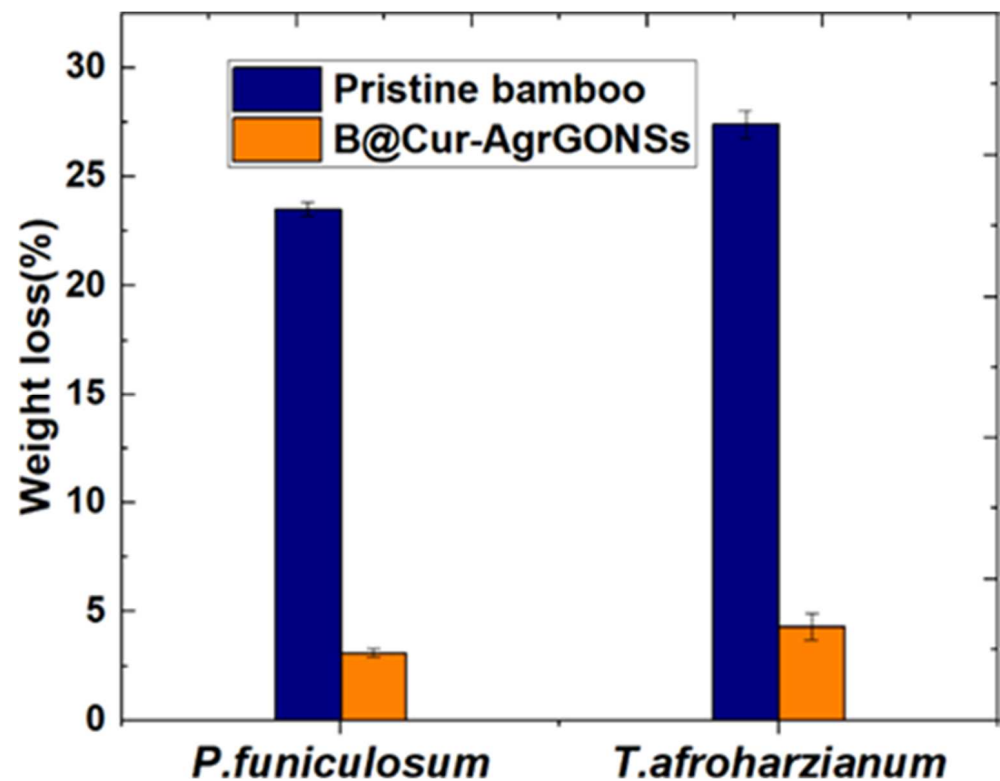
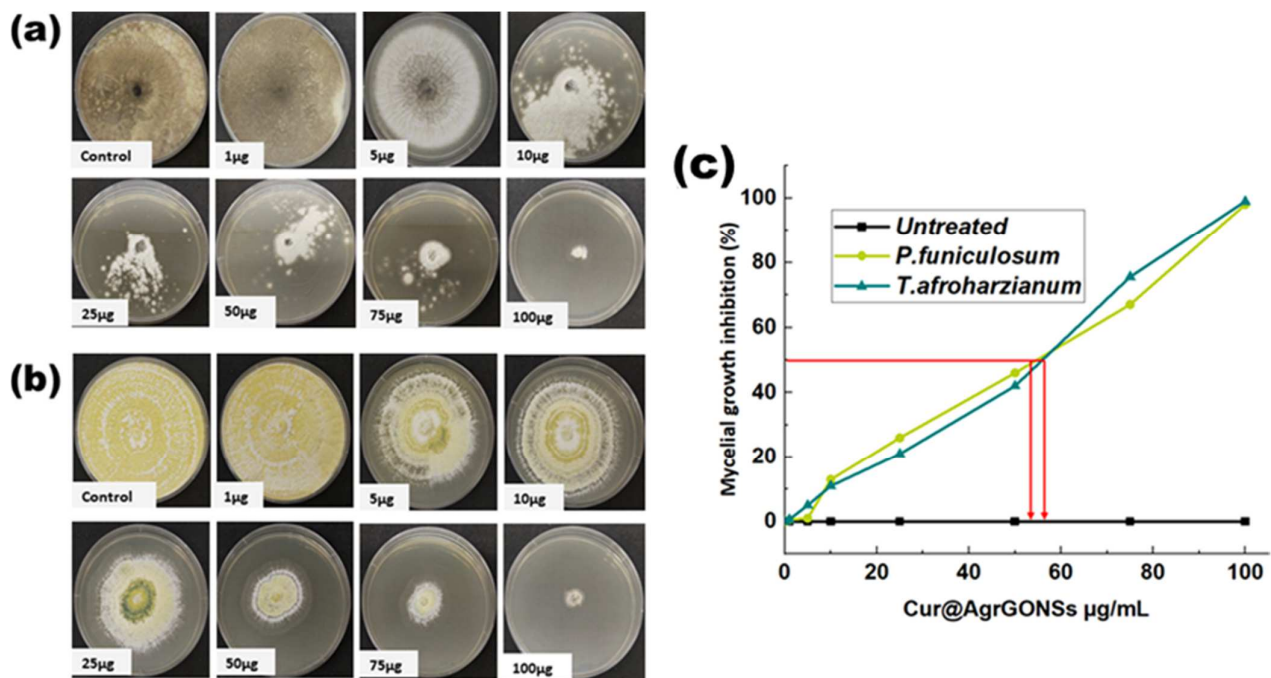


Figure 7. Average weight loss of pristine bamboo and B@Cur-AgrGONSs.

### 3.8. Antifungal Activity

The Cur-AgrGONSs effectively penetrated the bamboo, with this resulting in an antimicrobial coating agent. To completely inhibit mycelial growth, the concentration of Cur-AgrGONSs was determined to be 98 and 99  $\mu\text{g}/\text{mL}$  for *P. funiculosum* and *T. afroharzianum*, respectively (Figure 8a,b). This was likely due to direct contact between the fungi cell wall and the nanocomposites on the bamboo surface. The direct contact between a cell and the nanocomposites causes the reactive oxygen functionalities of the graphene nanocomposites to react chemically with the chitin and other polysaccharides organic functional groups on the fungi cell walls. The antimicrobial mechanism of graphene-based nanocomposites upon their direct exposure to microbes was previously reported [66]. Cur-AgrGONSs effectively inhibit fungi mycelium by being in direct contact with fungal cells. In addition, it was revealed that Cur-AgrGONSs interact with microorganisms by mechanically wrapping, intertwining with and damaging the cell membrane and finally causing the cell to die, which is a toxic function of Cur-AgrGONSs against phytopathogens.

In addition, half-maximal inhibitory concentration ( $\text{IC}_{50}$ ) values were calculated by plotting the concentration of Cur-AgrGONSs against the fungi mycelial growth inhibitory action in terms of percentages. Figure 8c clearly shows that the  $\text{IC}_{50}$  values of Cur-AgrGONSs was 54.6 and 55  $\mu\text{g}/\text{mL}$  against *P. funiculosum* and *T. afroharzianum*, respectively. This shows that the Cur-AgrGONSs have a superior inhibitory effect towards fungal pathogens, and this action might be because of the biofunctionalized nanosheets which were in direct contact with the pathogens, causing the pathogens to become wrapped by the nanosheets, which easily disrupted the integrity of the membranes of the cells [67].



**Figure 8.** (a) Mycelial growth of *T. afroharzianum* on media containing different concentrations of Cur-AgrGONSs (0–100 µg/mL); (b) Mycelial growth of *P. funiculosum* on media containing different concentrations of Cur-AgrGONSs (0–100 µg/mL); (c) Mycelial growth inhibition and determination of IC<sub>50</sub> value of Cur-AgrGONSs.

#### 4. Conclusions

This research focused on the application of nanotechnology in bamboo materials. The experimental findings of this research also contribute to a better understanding of the mechanisms of the efficient effect brought about by nano-incorporated bamboo. Green reduction is a unique field, especially in terms of the preparation of metals and metal oxide nanoparticles. A new type of bamboo coated with Cur-AgrGONSs was fabricated by using an immersion dry hydrothermal process. Bamboo coated with Cur-AgrGONSs improved its mold resistance and hydrophobicity. The possible synthesis and antibacterial mechanisms of Cur-AgrGONSs were discussed. The findings of this research revealed that fungal species interlocked with a thin sheet of Cur-AgrGONSs, aggregates, which damaged cell membrane integrity on a local level, which were involved in the mechanism of toxicity against fungal pathogens. Understanding the toxicity mechanisms of Cur-AgrGONSs on fungal isolates is extraordinarily useful in the context of retaining the shelf life of bamboo materials. The combination of GO nanosheets and silver nanoparticles resulted in improved antimicrobial properties and also improved the mechanical properties of the bamboo materials to a significant degree.

**Author Contributions:** Conceptualization, D.B. and C.-I.L.; investigation, D.B. and C.-I.L.; resources, C.-I.L.; data curation, D.B.; writing—original draft preparation, editing, D.B.; review and suggestions, C.-I.L.; supervision, C.-I.L.; project administration, C.-I.L.; funding acquisition, C.-I.L. All authors have read and agreed to the published version of the manuscript.

**Funding:** This research was funded by Ministry of Science and Technology (MOST), Taiwan, (MOST 108-2745-8-194-001).

**Institutional Review Board Statement:** Not applicable.

**Informed Consent Statement:** Not applicable.

**Data Availability Statement:** Data is contained within the article.

**Acknowledgments:** We are grateful to the Ministry of Science and Technology (MOST-108-2745-8-194-001), the Center for Nano Bio-Detection and The Featured Research Areas College Development Plan of National Chung Cheng University and the Advanced Institute of Manufacturing with High-tech Innovations (AIM-HI) and The Featured Areas Research Center Program within the framework of the Higher Education Sprout Project of the Ministry of Education (MOE) in Taiwan for financial support.

**Conflicts of Interest:** The authors declare no conflict of interest.

## References

1. Wahab, R.; Sudin, M.; Samsi, H.W. Fungal Colonisation and Decay in Tropical Bamboo Species. *Appl. Sci.* **2005**, *5*, 897–902. [[CrossRef](#)]
2. Scurlock, J.M.; Dayton, D.C.; Hames, B. Bamboo: An overlooked biomass resource. *Biomass Bioenergy* **2000**, *19*, 229–244. [[CrossRef](#)]
3. Song, W.; Zhang, K.; Chen, Z.; Hong, G.; Lin, J.; Hao, C.; Zhang, S. Effect of xylanase–laccase synergistic pretreatment on physical–mechanical properties of environment-friendly self-bonded bamboo particleboards. *J. Polym. Environ.* **2018**, *26*, 4019–4033. [[CrossRef](#)]
4. Jain, S.; Kumar, R.; Jindal, U.C. Mechanical behaviour of bamboo and bamboo composite. *J. Mater. Sci.* **1992**, *27*, 4598–4604. [[CrossRef](#)]
5. Gugnani, H.C.; Paliwal-Joshi, A.; Rahman, H.; Padhye, A.A.; Singh, T.S.K.; Das, T.K.; Khanal, B.; Bajaj, R.; Rao, S.; Chukhani, R. Occurrence of pathogenic fungi in soil of burrows of rats and of other sites in bamboo plantations in India and Nepal. *Mycoses* **2007**, *50*, 507–511. [[CrossRef](#)]
6. Hamed, S.A.M. In vitro studies on wood degradation in soil by soft-rot fungi: *Aspergillus niger* and *Penicillium chrysogenum*. *Int. Biodeterior. Biodegrad.* **2013**, *78*, 98–102. [[CrossRef](#)]
7. Wu, H.; Yang, X.; Rao, J.; Zhang, Y.; Sun, F. Improvement of bamboo properties via in situ construction of polyhydroxyethyl methylacrylate and polymethyl methylacrylate networks. *Bioresources* **2018**, *13*, 6–14. [[CrossRef](#)]
8. Fei, P.; Xiong, H.; Cai, J.; Liu, C.; Yu, Y. Enhanced the weatherability of bamboo fiber-based outdoor building decoration materials by rutile nano-TiO<sub>2</sub>. *Constr. Build. Mater.* **2016**, *114*, 307–316. [[CrossRef](#)]
9. Agnihotri, S.; Mukherji, S.; Mukherji, S. Size-controlled silver nanoparticles synthesized over the range 5–100 nm using the same protocol and their antibacterial efficacy. *RSC Adv.* **2014**, *4*, 3974–3983. [[CrossRef](#)]
10. Sarmast, M.K.; Salehi, H. Silver nanoparticles: An influential element in plant nanobiotechnology. *Mol. Biotechnol.* **2016**, *58*, 441–449. [[CrossRef](#)]
11. Chang, S.T.; Yeh, T.F. Protection and fastness of green color of moso bamboo (*Phyllostachys pubescens* Mazel) treated with chromium-based reagents. *J. Wood Sci.* **2001**, *47*, 228–232. [[CrossRef](#)]
12. Chang, S.T.; Wu, J.H. Green-color conservation of ma bamboo (*Dendrocalamus latiflorus*) treated with chromium-based reagents. *J. Wood Sci.* **2000**, *46*, 40–44. [[CrossRef](#)]
13. Yu, Y.; Jiang, Z.; Wang, G.; Tian, G.; Wang, H.; Song, Y. Surface functionalization of bamboo with nanostructured ZnO. *Wood Sci. Technol.* **2012**, *46*, 781–790. [[CrossRef](#)]
14. Marcano, D.C.; Kosynkin, D.V.; Berlin, J.M.; Sinitskii, A.; Sun, Z.; Slesarev, A.; Alemany, L.B.; Lu, W.; Tour, J.M. Improved synthesis of graphene oxide. *ACS Nano* **2010**, *4*, 4806–4814. [[CrossRef](#)]
15. Mosselhy, D.A.; Abd El-Aziz, M.; Hanna, M.; Ahmed, M.A.; Husien, M.M.; Feng, Q. Comparative synthesis and antimicrobial action of silver nanoparticles and silver nitrate. *J. Nanopart. Res.* **2015**, *17*, 473. [[CrossRef](#)]
16. Liu, S.; Zeng, T.H.; Hofmann, M.; Burcombe, E.; Wei, J.; Jiang, R.; Kong, J.; Chen, Y. Antibacterial activity of graphite, graphite oxide, graphene oxide, and reduced graphene oxide: Membrane and oxidative stress. *ACS Nano* **2011**, *5*, 6971–6980. [[CrossRef](#)]
17. Shao, W.; Liu, X.; Min, H.; Dong, G.; Feng, Q.; Zuo, S. Preparation, characterization, and antibacterial activity of silver nanoparticle-decorated graphene oxide nanocomposite. *ACS Appl. Mater. Interfaces* **2015**, *7*, 6966–6973. [[CrossRef](#)]
18. Li, C.; Wang, X.; Chen, F.; Zhang, C.; Zhi, X.; Wang, K.; Cui, D. The antifungal activity of graphene oxide–silver nanocomposites. *Biomaterials* **2013**, *34*, 3882–3890. [[CrossRef](#)]
19. Tang, J.; Chen, Q.; Xu, L.; Zhang, S.; Feng, L.; Cheng, L.; Xu, H.; Liu, Z.; Peng, R. Graphene oxide–silver nanocomposite as a highly effective antibacterial agent with species-specific mechanisms. *ACS Appl. Mater. Interfaces* **2013**, *5*, 3867–3874. [[CrossRef](#)]
20. Kim, S.W.; Jung, J.H.; Lamsal, K.; Kim, Y.S.; Min, J.S.; Lee, Y.S. Antifungal effects of silver nanoparticles (AgNPs) against various plant pathogenic fungi. *Mycobiology* **2012**, *40*, 53–58. [[CrossRef](#)]
21. Palmieri, V.; Bugli, F.; Cacaci, M.; Perini, G.; Maio, F.D.; Delogu, G.; Torelli, R.; Conti, C.; Sanguinetti, M.; Spirito, M.D.; et al. Graphene oxide coatings prevent *Candida albicans* biofilm formation with a controlled release of curcumin-loaded nanocomposites. *Nanomedicine* **2018**, *13*, 2867–2879. [[CrossRef](#)]
22. Kim, S.W.; Kim, K.S.; Lamsal, K.; Kim, Y.J.; Kim, S.B.; Jung, M.; Sim, S.J.; Kim, H.S.; Chang, S.J.; Kim, J.K.; et al. An in vitro study of the antifungal effect of silver nanoparticles on oak wilt pathogen *Raffaelea* sp. *J. Microbiol. Biotechnol.* **2009**, *19*, 760–764. [[CrossRef](#)] [[PubMed](#)]
23. Yilmaz, A.; Bozkurt, F.; Cicek, P.K.; Dertli, E.; Durak, M.Z.; Yilmaz, M.T. A novel antifungal surface-coating application to limit postharvest decay on coated apples: Molecular, thermal and morphological properties of electrospun zein–nanofiber mats loaded with curcumin. *Innov. Food Sci. Emerg. Technol.* **2016**, *37*, 74–83. [[CrossRef](#)]

24. Casado-Sanz, M.M.; Silva-Castro, I.; Ponce-Herrero, L.; Martín-Ramos, P.; Martín-Gil, J.; Acuña-Rello, L. White-rot fungi control on *Populus* spp. wood by pressure treatments with silver nanoparticles, chitosan oligomers and propolis. *Forests* **2019**, *10*, 885. [[CrossRef](#)]
25. Akhtari, M.; Arefkhani, M. Study of microscopy properties of wood impregnated with nanoparticles during exposed to white-rot fungus. *Agric. Sci. Dev.* **2013**, *2*, 116–119.
26. Shen, J.; Shi, M.; Yan, B.; Ma, H.; Li, N.; Ye, M. One-pot hydrothermal synthesis of Ag-reduced graphene oxide composite with ionic liquid. *J. Mater. Chem.* **2011**, *21*, 7795–7801. [[CrossRef](#)]
27. Wang, J.; Sun, Q.; Sun, F.; Zhang, Q.; Jin, C. Layer-by-layer self-assembly of reduced graphene oxide on bamboo timber surface with improved decay resistance. *Eur. J. Wood Wood Prod.* **2018**, *76*, 1223–1231. [[CrossRef](#)]
28. Ferreira, F.D.; Mossini, S.A.G.; Ferreira, F.M.D.; Arrotéia, C.C.; da Costa, C.L.; Nakamura, C.V.; Machinski Junior, M. The inhibitory effects of *Curcuma longa* L. essential oil and curcumin on *Aspergillus flavus* link growth and morphology. *Sci. World J.* **2013**, *2013*, 343804. [[CrossRef](#)]
29. Abidin, Z.H.Z.; Naziron, N.N.; Nasir, K.M.; Rusli, M.S.; Lee, S.V.; Kufian, M.Z.; Majid, S.R.; Vengadaesvaran, B.; Arof, A.K.; Taha, R.M.; et al. Influence of curcumin natural dye colorant with PMMA-acrylic polyol blended polymer. *Pigment. Resin Technol.* **2013**, *42*, 95–102. [[CrossRef](#)]
30. Necolau, M.I.; Pandeale, A.M. Recent advances in graphene oxide-based anticorrosive coatings: An overview. *Coatings* **2020**, *10*, 1149. [[CrossRef](#)]
31. Wang, Y.; Li, Y.; Xue, S.; Zhu, W.; Wang, X.; Huang, P.; Fu, S. Superstrong, lightweight, and exceptional environmentally stable SiO<sub>2</sub>@GO/bamboo composites. *ACS Appl. Mater. Interfaces* **2022**, *14*, 11–20. [[CrossRef](#)] [[PubMed](#)]
32. Li, J.; Ren, D.; Wu, Z.; Huang, C.; Yang, H.; Chen, Y.; Yu, H. Visible-light-mediated antifungal bamboo based on Fe-doped TiO<sub>2</sub> thin films. *RSC Adv.* **2017**, *7*, 55131–55140. [[CrossRef](#)]
33. Liu, G.; Lu, Z.; Zhu, X.; Du, X.; Hu, J.; Chang, S.; Li, X.; Liu, Y. Facile in-situ growth of Ag/TiO<sub>2</sub> nanoparticles on polydopamine modified bamboo with excellent mildew-proofing. *Sci. Rep.* **2019**, *9*, 16496. [[CrossRef](#)] [[PubMed](#)]
34. Li, J.; Su, M.; Wang, A.; Wu, Z.; Chen, Y.; Qin, D.; Jiang, Z. In situ formation of Ag nanoparticles in mesoporous TiO<sub>2</sub> films decorated on bamboo via self-sacrificing reduction to synthesize nanocomposites with efficient antifungal activity. *Int. J. Mol. Sci.* **2019**, *20*, 5497. [[CrossRef](#)]
35. Yu, H.; Du, C.; Liu, H.; Wei, J.; Zhou, Z.; Huang, Q.; Yao, X. Preparation and characterization of bamboo strips impregnation treated by silver-loaded thermo-sensitive nanogels. *Bioresources* **2017**, *12*, 8390–8401. [[CrossRef](#)]
36. Wang, D.; Hu, C.; Gu, J.; Tu, D.; Wang, G.; Jiang, M.; Zhang, W. Bamboo surface coated with polymethylsilsesquioxane/Cu-containing nanoparticles (PMS/CuNP) xerogel for superhydrophobic and anti-mildew performance. *J. Wood Sci.* **2020**, *66*, 33. [[CrossRef](#)]
37. Lou, Z.; Han, X.; Liu, J.; Ma, Q.; Yan, H.; Yuan, C.; Yang, L.; Han, H.; Weng, F.; Li, Y. Nano-Fe<sub>3</sub>O<sub>4</sub>/bamboo bundles/phenolic resin-oriented recombination ternary composite with enhanced multiple functions. *Compos. B Eng.* **2021**, *226*, 109335. [[CrossRef](#)]
38. Li, J.; Wu, Z.; Bao, Y.; Chen, Y.; Huang, C.; Li, N.; He, S.; Chen, Z. Wet chemical synthesis of ZnO nanocoating on the surface of bamboo timber with improved mould-resistance. *J. Saudi Chem. Soc.* **2017**, *21*, 920–928. [[CrossRef](#)]
39. Chen, J.; Ma, Y.; Lin, H.; Zheng, Q.; Zhang, X.; Yang, W.; Li, R. Fabrication of hydrophobic ZnO/PMHS coatings on bamboo surfaces: The synergistic effect of ZnO and PMHS on anti-mildew properties. *Coatings* **2018**, *9*, 15. [[CrossRef](#)]
40. Ren, D.; Li, J.; Xu, J.; Wu, Z.; Bao, Y.; Li, N.; Chen, Y. Efficient antifungal and flame-retardant properties of ZnO-TiO<sub>2</sub>-layered double-nanostructures coated on bamboo substrate. *Coatings* **2018**, *8*, 341. [[CrossRef](#)]
41. Pandoli, O.; Martini, R.D.S.; Romani, E.C.; Paciornik, S.; Mauricio, M.H.D.P.; Alves, H.D.L.; Pereira-Meirelles, F.V.; Luz, E.L.; Koller, S.M.L.; Valiente, H.; et al. Colloidal silver nanoparticles: An effective nano-filler material to prevent fungal proliferation in bamboo. *RSC Adv.* **2016**, *6*, 98325–98336. [[CrossRef](#)]
42. Debnath, S.; Karmakar, P.; Bhattacharjee, S.; Majumdar, K.; Das, P.; Saha, A.K. Isolation and identification of fungal assemblages in the necrotic spots of *Bambusa pallida* (L.) Voss. *Annu. Plant Sci.* **2018**, *7*, 2160–2165. [[CrossRef](#)]
43. Kim, J.J.; Lee, S.S.; Ra, J.B.; Lee, H.; Huh, N.; Kim, G.H. Fungi associated with bamboo and their decay capabilities. *Holzforchung* **2011**, *65*, 271–275. [[CrossRef](#)]
44. Gardes, M.; Bruns, T.D. ITS primers with enhanced specificity for basidiomycetes-application to the identification of mycorrhizae and rusts. *Mol. Ecol.* **1993**, *2*, 113–118. [[CrossRef](#)] [[PubMed](#)]
45. Morakotkarn, D.; Kawasaki, H.; Seki, T. Molecular diversity of bamboo-associated fungi isolated from Japan. *FEMS Microbiol. Lett.* **2007**, *266*, 10–19. [[CrossRef](#)] [[PubMed](#)]
46. Hummers Jr, W.S.; Offeman, R.E. Preparation of graphitic oxide. *J. Am. Chem. Soc.* **1958**, *80*, 1339. [[CrossRef](#)]
47. Sun, F.; Bao, B.; Ma, L.; Chen, A.; Duan, X. Mould-resistance of bamboo treated with the compound of chitosan-copper complex and organic fungicides. *J. Wood Sci.* **2012**, *58*, 51–56. [[CrossRef](#)]
48. Yang, H.; Deng, Y. Preparation and physical properties of superhydrophobic papers. *J. Colloid Interface Sci.* **2008**, *325*, 588–593. [[CrossRef](#)]
49. Jin, C.; Li, J.; Han, S.; Wang, J.; Sun, Q. A durable, superhydrophobic, superoleophobic and corrosion-resistant coating with rose-like ZnO nanoflowers on a bamboo surface. *Appl. Surf. Sci.* **2014**, *320*, 322–327. [[CrossRef](#)]
50. Li, J.; Sun, Q.; Yao, Q.; Wang, J.; Han, S.; Jin, C. Fabrication of robust superhydrophobic bamboo based on ZnO nanosheet networks with improved water-, UV-, and fire-resistant properties. *J. Nanomater.* **2015**, *2015*, 431426. [[CrossRef](#)]

51. ASTM D2017-05; Standard Method of Accelerated Laboratory Test of Natural Decay Resistance of Wood. American Society for Testing and Materials: West Conshohocken, PA, USA, 2008.
52. Cloutier, M.; Mantovani, D.; Rosei, F. Antibacterial coatings: Challenges, perspectives, and opportunities. *Trends Biotechnol.* **2015**, *33*, 637–652. [[CrossRef](#)] [[PubMed](#)]
53. Wei, D.; Schmidt, O.; Liese, W. Method to test fungal degradation of bamboo and wood using vermiculite as reservoir for moisture and nutrients. *Maderas-Cienc. Tecnol.* **2013**, *15*, 349–356. [[CrossRef](#)]
54. Kordali, S.; Cakir, A.; Ozer, H.; Cakmakci, R.; Kesdek, M.; Mete, E. Antifungal, phytotoxic and insecticidal properties of essential oil isolated from Turkish *Origanum acutidens* and its three components, carvacrol, thymol and p-cymene. *Bioresour. Technol.* **2008**, *99*, 8788–8795. [[CrossRef](#)] [[PubMed](#)]
55. Sun, Q.; Yu, H.; Liu, Y.; Li, J.; Cui, Y.; Lu, Y. Prolonging the combustion duration of wood by TiO<sub>2</sub> coating synthesized using cosolvent-controlled hydrothermal method. *J. Mater. Sci.* **2010**, *45*, 6661–6667. [[CrossRef](#)]
56. Desai, R.; Mankad, V.; Gupta, S.K.; Jha, P.K. Size distribution of silver nanoparticles: UV-visible spectroscopic assessment. *Nanosci. Nanotechnol. Lett.* **2012**, *4*, 30–34. [[CrossRef](#)]
57. Andersson, S.; Serimaa, R.; Paakkari, T.; Saranpaa, P.; Pesonen, E. Crystallinity of wood and the size of cellulose crystallites in Norway spruce (*Picea abies*). *J. Wood Sci.* **2003**, *49*, 531–537. [[CrossRef](#)]
58. Li, J.; Zheng, H.; Sun, Q.; Han, S.; Fan, B.; Yao, Q.; Yan, C.; Jin, C. Fabrication of superhydrophobic bamboo timber based on an anatase TiO<sub>2</sub> film for acid rain protection and flame retardancy. *RSC Adv.* **2015**, *5*, 62265–62272. [[CrossRef](#)]
59. Wang, G.; Yang, J.; Park, J.; Gou, X.; Wang, B.; Liu, H.; Yao, J. Facile synthesis and characterization of graphene nanosheets. *J. Phys. Chem. C* **2008**, *112*, 8192–8195. [[CrossRef](#)]
60. Caccia, M.; Giuranno, D.; Molina-Jorda, J.M.; Moral, M.; Nowak, R.; Ricci, E.; Sobczak, N.; Narciso, J.; Fernández Sanz, J. Graphene translucency and interfacial interactions in the Gold/Graphene/SiC system. *J. Phys. Chem.* **2018**, *9*, 3850–3855. [[CrossRef](#)]
61. Dinh, D.A.; Hui, K.S.; Hui, K.N.; Cho, Y.R.; Zhou, W.; Hong, X.; Chun, H.H. Green synthesis of high conductivity silver nanoparticle-reduced graphene oxide composite films. *Appl. Surf. Sci.* **2014**, *298*, 62–67. [[CrossRef](#)]
62. Chen, J.; Zheng, X.; Wang, H.; Zheng, W. Graphene oxide-Ag nanocomposite: In situ photochemical synthesis and application as a surface-enhanced Raman scattering substrate. *Thin Solid Films* **2011**, *520*, 179–185. [[CrossRef](#)]
63. ISO 13061-1; Physical and Mechanical Properties of Wood—Test Methods for Small Clear Wood Specimens—Part 1: Determination of Moisture Content for Physical and Mechanical Tests. International Organization for Standardization: Geneva, Switzerland, 2014.
64. Lu, Y.; Xiao, S.; Gao, R.; Li, J.; Sun, Q. Improved weathering performance and wettability of wood protected by CeO<sub>2</sub> coating deposited onto the surface. *Holzforschung* **2014**, *68*, 345–351. [[CrossRef](#)]
65. Peng, Y.; Wu, S. The structural and thermal characteristics of wheat straw hemicellulose. *J. Anal. Appl. Pyrolysis* **2010**, *88*, 134–139. [[CrossRef](#)]
66. Akhavan, O.; Ghaderi, E. Toxicity of graphene and graphene oxide nanowalls against bacteria. *ACS Nano* **2010**, *4*, 5731–5736. [[CrossRef](#)] [[PubMed](#)]
67. Chen, J.; Peng, H.; Wang, X.; Shao, F.; Yuan, Z.; Han, H. Graphene oxide exhibits broad-spectrum antimicrobial activity against bacterial phytopathogens and fungal conidia by intertwining and membrane perturbation. *Nanoscale* **2014**, *6*, 1879–1889. [[CrossRef](#)]